MATERIALS SCIENCE

Bose-Einstein condensation superconductivity induced by disappearance of the nematic state

Takahiro Hashimoto[1], Yuichi Ota[1], Akihiro Tsuzuki[1], Tsubaki Nagashima[1], Akiko Fukushima[1], Shigeru Kasahara[2], Yuji Matsuda[2], Kohei Matsuura[3], Yuta Mizukami[3], Takasada Shibauchi[3], Shik Shin[4,5], Kozo Okazaki[1,5,6]*

The crossover from the superconductivity of the Bardeen-Cooper-Schrieffer (BCS) regime to the Bose-Einstein condensation (BEC) regime holds a key to understanding the nature of pairing and condensation of fermions. It has been mainly studied in ultracold atoms, but in solid systems, fundamentally previously unknown insights may be obtained because multiple energy bands and coexisting electronic orders strongly affect spin and orbital degrees of freedom. Here, we provide evidence for the BCS-BEC crossover in iron-based superconductors $FeSe_{1-x}S_x$ from laser-excited angle-resolved photoemission spectroscopy. The system enters the BEC regime with $x = 0.21$, where the nematic state that breaks the orbital degeneracy is fully suppressed. The substitution dependence is opposite to the expectation for single-band superconductors, which calls for a new mechanism of BCS-BEC crossover in this system.

INTRODUCTION

Weak-coupling Bardeen-Cooper-Schrieffer (BCS) pairing and strong-coupling Bose-Einstein condensation (BEC) are connected continuously through the BCS-BEC crossover regime as canonically shown in Fig. 1A (*1*). This regime holds a key to understanding the nature of pairing and condensation of particles. To tune across the BCS-BEC crossover, it is necessary to control attractive interaction between two fermions. In ultracold atomic systems, this tuning is achieved by applying an external magnetic field via Feshbach resonance. Realization of the BCS-BEC crossover in an electron system of a solid is desired for several reasons: (i) The phase diagram may be strongly modified by the underlying properties of solids, for example, multiple energy bands and other electronic degrees of freedom such as orbitals and spins. (ii) The ratio of the superconducting (SC) critical temperature T_c to the Fermi temperature T_F, T_c/T_F ($\sim\Delta/\varepsilon_F$, where Δ and ε_F are the SC gap and the Fermi energy, respectively) is expected to be large ($\Delta/\varepsilon_F \sim 1$) in this regime. BEC superconductivity can be regarded as "high-temperature" superconductivity in the sense that T_c is comparable to T_F. (iii) The electronic structure in the SC state is expected to be different from the usual Bogoliubov quasiparticle (BQP) band dispersion. In the weak-coupling BCS regime, the dispersion of the BQP shows the characteristic back-bending near k_F, which is downward convex around $k = 0$ in the case of a hole band below E_F, as shown in Fig. 1B, where k is the crystal momentum of electrons. On the other hand, in the strong-coupling BEC regime, the dispersion with a minimum gap at $k = 0$ is expected, which is upward convex around $k = 0$ in the case of a hole band below E_F, as shown in Fig. 1D. In the crossover regime, the BQP dispersion is intermediate between two extreme cases and the flat dispersion appears. Despite interest in the subject, identifying the BCS-BEC crossover in a solid has been elusive, because it is difficult to control the pairing interaction between electrons. To investigate the realization of the BCS-BEC crossover, Δ/ε_F can be used as a measure of the pairing strength: Δ/ε_F increases as a system approaches the BEC regime, and it becomes unity in the crossover regime, where a pseudogap is expected to open at a temperature higher than T_c as a result of preformed bosonic pairs, as shown in Fig. 1A.

Several Fe-based superconductors have been proposed as candidate materials that exhibit the BCS-BEC crossover. In $Ba_{1-x}K_xFe_2As_2$, flat band dispersion and $\Delta/\varepsilon_F \sim 1$ have been observed around the M point in the Brillouin zone (*2*), and in $LiFe_{1-x}Co_xAs$, $\Delta/\varepsilon_F \sim 1$ has been reported (*3*). In $Fe_{1+y}Se_xTe_{1-x}$, it has been reported that the BQP band dispersion changes from downward convex as in the BCS regime to a flat band as in the crossover regime, and Δ/ε_F increases by changing the concentration of excess Fe (*4*, *5*). Although $\Delta/\varepsilon_F \sim 1$ and flat bands have been observed in these compounds, it is not clear whether all the bands at E_F exhibit the same behavior, and systematic evidence together with the observation of a pseudogap is still absent.

Among iron-based superconductors, $FeSe_{1-x}S_x$ is one of the most promising systems to investigate the BCS-BEC crossover. A parent compound FeSe (*6*) exhibits superconductivity at $T_c \sim 10$ K. Its Δ/ε_F has been reported to be close to unity at all the bands at E_F, suggesting that FeSe is in the BCS-BEC crossover regime (*7*). However, there are disagreements in the behaviors expected from the BCS-BEC crossover regime. Whereas one group has reported that strong SC fluctuations are observed, which may be related to the presence of preformed pairs (*8*), another group has reported the absence of such strong fluctuations (*9*). The existence of a pseudogap, which is a signature of preformed pairs, has been reported using nuclear magnetic resonance (*8*, *10*) and scanning tunneling spectroscopy (STS) measurements (*11*), but its absence has been reported using STS recently (*12*). In a substituted system $FeSe_{1-x}S_x$, as x increases, the structural transition (from a tetragonal phase to an orthorhombic phase) is suppressed, and the quantum critical point (QCP) of the nematic (unidirectional) electronic fluctuation is observed at $x_c \sim 0.17$ according to elastoresistivity measurements (*13*). At this QCP, an abrupt change of the SC state has been observed (*14*, *15*). However, it is not understood how BCS-BEC crossover develops as x increases or how nematicity is related in the $FeSe_{1-x}S_x$ system.

[1]Institute for Solid State Physics (ISSP), The University of Tokyo, Kashiwa, Chiba 277-8581, Japan. [2]Department of Physics, Kyoto University, Kyoto 606-8502, Japan. [3]Department of Advanced Materials Science, The University of Tokyo, Kashiwa, Chiba 277-8561, Japan. [4]Office of University Professor, The University of Tokyo, Kashiwa, Chiba 277-8568, Japan. [5]Material Innovation Research Center, The University of Tokyo, Kashiwa, Chiba 277-8561, Japan. [6]Trans-scale Quantum Science Institute, The University of Tokyo, Bunkyo-ku, Tokyo 113-0033, Japan.
*Corresponding author. Email: okazaki@issp.u-tokyo.ac.jp

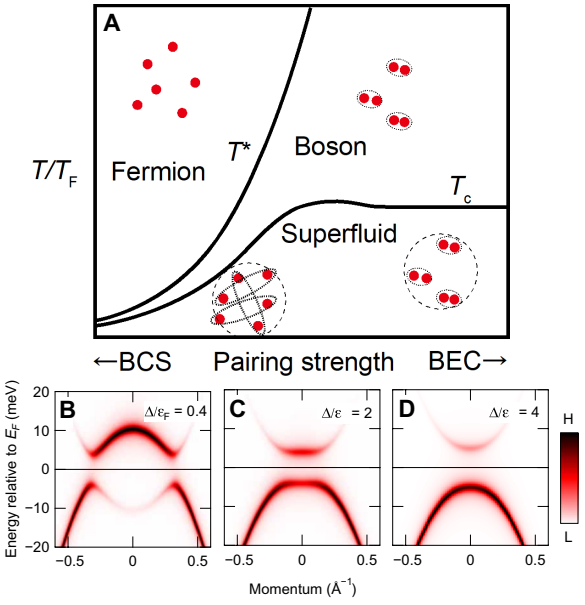

Fig. 1. Phase diagram of the BCS-BEC crossover and BQP band dispersions. (**A**) Canonical phase diagram of BCS-BEC crossover. T_c and T^* are condensation and pairing temperatures, respectively. As the pairing strength increases, T^* and T_c become separate, and a pseudogap is expected at $T^* > T > T_c$. (**B** to **D**) BQP band dispersions in the BCS regime, the crossover regime, and the BEC regime, respectively. The dispersion is downward convex around $k = 0$ for the BCS regime, becomes flat in the crossover regime, and then becomes upward convex in the BEC regime, because of the chemical potential shift (*4*, *20*). Δ/ε_F is referred to as a measure of the pairing strength for single-band superconductors.

In this study, we have performed laser-excited angle-resolved photoemission spectroscopy (ARPES) on $FeSe_{1-x}S_x$ (where $x = 0$ to 0.21) around the Brillouin zone center and systematically investigated the band dispersions in the SC state, the existence of a pseudogap above T_c, and the values of Δ/ε_F to obtain complete and systematic evidence of the BCS-BEC crossover in an electron system in a solid. We observe that BQP dispersion in the SC state exhibits a systematic change from a downward convex shape to an upward convex one as x increases. Also, we observe a pseudogap above T_c for $x = 0.21$, whereas it is absent for $x = 0$ and 0.13. This systematic variation of the band structure and the existence of a pseudogap should be regarded as complete evidence that $FeSe_{1-x}S_x$ can be controlled from the BCS regime to the BEC regime by increasing x. However, in contrast to the expectation from the single-band calculation, the estimated value of Δ/ε_F decreases as the system moves toward the BEC regime. We point out a possibility that the system enters the BEC regime as a result of the interband coupling between the BQP band and a hole band below E_F, which is controlled by nematicity.

RESULTS

Band dispersions in the SC state

First, we show the sulfur substitution dependence of the band dispersions in the SC state. Figure 2 (A to E) shows the ARPES intensity plots of $FeSe_{1-x}Se_x$ (where $x = 0$, 0.04, 0.13, 0.16, and 0.21) taken in the SC state with *s*-polarized light. The detailed band assignments and the effect of nematicity are described in fig. S1. To see the BQP band dispersions more clearly, we show enlarged plots around E_F in Fig. 2 (F to J). We have plotted the BQP band dispersions determined from the energy distribution curves (EDCs) of each composition as indicated by red markers. From these plots, we can see that the BQP band dispersion, which is downward convex at $x = 0$, systematically changes and becomes flat at $x = 0.16$; it then, eventually, becomes upward convex at $x = 0.21$. This systematic change is consistent with that expected from the chemical potential shift in the BCS-BEC crossover, as shown in Fig. 1 (B to D), and thus strongly suggests that $FeSe_{1-x}S_x$ is tuned from the BCS-BEC crossover regime ($x = 0$) to the BEC regime ($x = 0.21$). Note that the BQP band dispersion at $x = 0$ is much flatter than in the case for the BCS regime, which shows that it is already in the crossover regime (see fig. S2 for details).

Emergence of the pseudogap

To obtain complete evidence for the BCS-BEC crossover, we have investigated the existence of a pseudogap. Figure 3 shows the temperature-dependent EDCs at k_F and the EDCs symmetrized with respect to E_F for $x = 0$, 0.13, and 0.21. To see the temperature dependence more clearly, the symmetrized EDCs have been divided by that at 25 K. For $x = 0$ and 0.13, one can see that SC coherent peaks grow below $T_c \sim 10$ K, as shown in Fig. 3 (A to D), and this demonstrates that the samples are sufficiently cooled to observe the SC states and that the energy resolution is high enough. In contrast to $x = 0$ and 0.13, for $x = 0.21$, one can recognize that the intensity of the EDCs around E_F starts to decrease from $T^* \sim 15$ K with decreasing temperature, although T_c of this composition is as low as ~4 K. Because the amount of sulfur substitution is relatively large, impurity scattering may be substantial for this composition ($x = 0.21$). However, because the scattering rate resulting from impurities should be independent of temperature, the decreasing intensity at E_F above T_c strongly suggests that a pseudogap definitely exists for $x = 0.21$. We note that the pseudogap could emerge as a correlated electronic state independent from the BCS-BEC crossover, and several exotic phases have been proposed for the pseudogap state in underdoped cuprates (*16*). In the present case with the BEC-like dispersion in the SC state, however, it should be more natural to associate it with the BCS-BEC crossover because the phase diagram shown in Fig. 1A implies the deviation of pairing temperature from the actual T_c. Whereas T_c is as low as ~ 4 K for $x = 0.21$, the pseudogap appears at $T^* \sim 15$ K. This means that T^* is almost a factor of 4 greater than T_c. This may suggest that $x = 0.21$ is located deep inside the BEC regime in the phase diagram shown in Fig. 1A. The signature of the flat band appears below T^*, corresponding to the pseudogap (see fig. S5 for details).

Substitution dependence of Δ/ε_F

We have confirmed that the BQP dispersion changes from a downward convex to an upward convex shape with increasing x of $FeSe_{1-x}S_x$, and that the pseudogap appears at $T^* \sim 4T_c$ for $x = 0.21$. These observations strongly suggest that, as x increases, the system approaches the BEC regime. We next discuss the substitution dependence of Δ/ε_F, a conventional measure of the pairing strength. As discussed in Fig. 1, Δ/ε_F is expected to get close to unity at the BCS-BEC crossover regime. We evaluate ε_F from the dispersions of each sample. We show the ARPES intensity plots of FeSe ($x = 0$) taken with *s*- and *p*-polarized light at 25 K ($T > T_c$) in Fig. 4 (A and B, respectively). These images show the hole-like dispersions at different

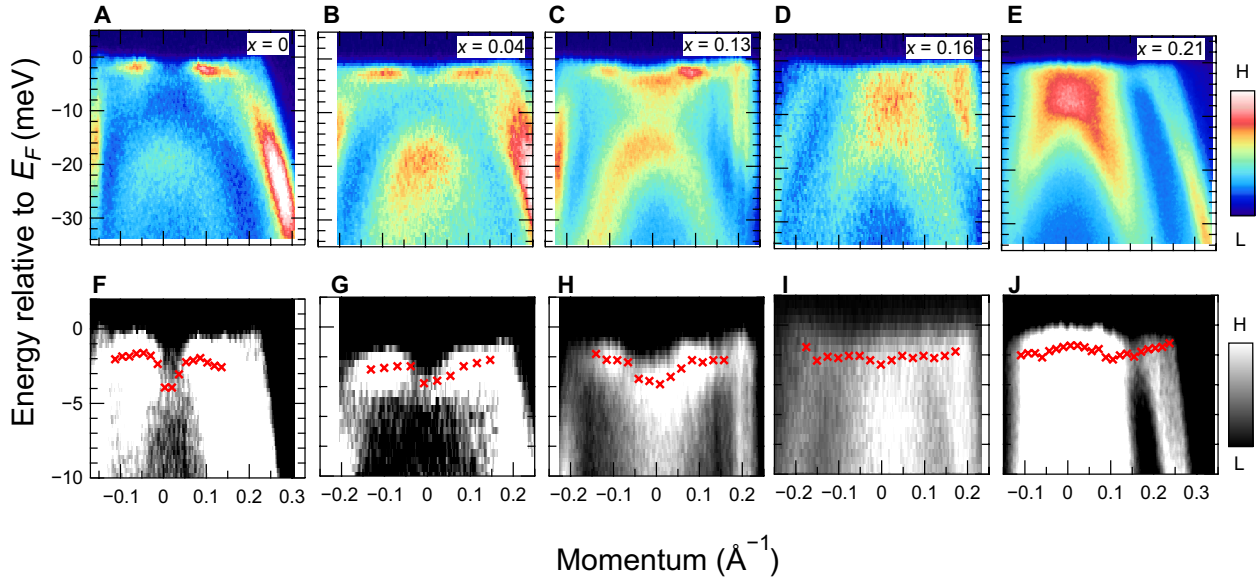

Fig. 2. ARPES intensity plots of $FeSe_{1-x}S_x$ along the Γ–*M* direction measured in the SC state. (**A** to **E**) ARPES intensity plots of $x = 0$, 0.04, 0.13, 0.16, and 0.21 along the Γ – *M* direction taken at 2 K with *s*-polarized incident light. (**F** to **J**) Enlarged plots of (A) to (E). The red markers represent the BQP band dispersions determined from the energy distribution curves.

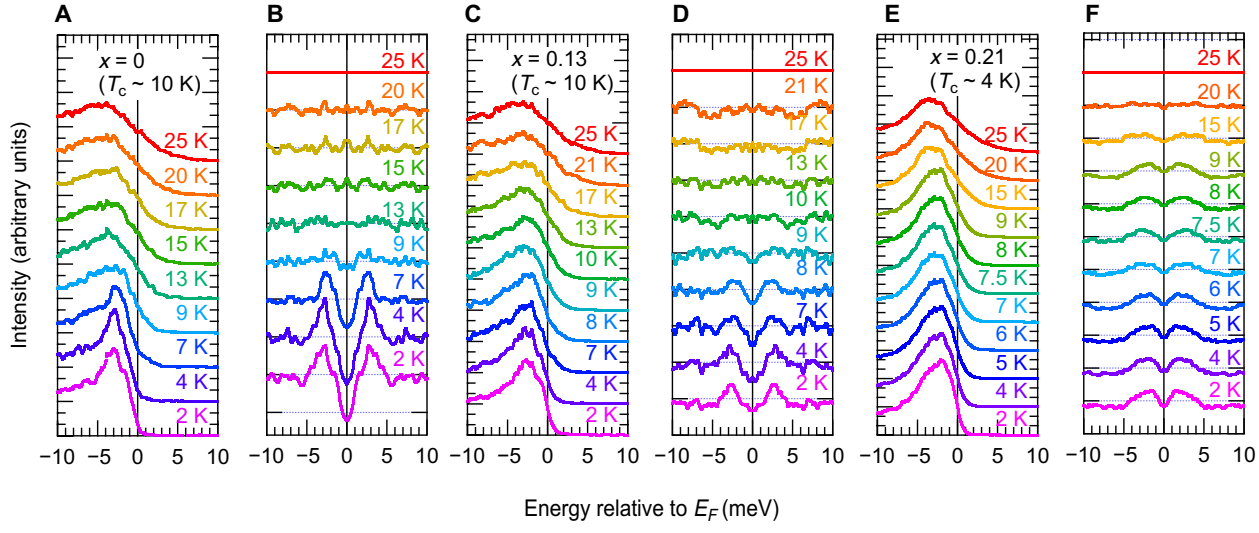

Fig. 3. EDCs of $FeSe_{1-x}S_x$ at $k = k_F$ taken with *p*-polarized light. (**A**, **C**, and **E**) Temperature dependence of the raw EDCs at $k = k_F$ for $x = 0$, 0.13, and 0.21, respectively. (**B**, **D**, and **F**) EDCs in (A), (C), and (E) symmetrized at $E = E_F$ and divided by that at 25 K, respectively. Each EDC has been equally offset for clarity.

momentum positions around E_F. As described in fig. S1, two elliptical Fermi surfaces (FSs) are overlapped as a result of twinning of the orthorhombic crystal (*17*). The dispersions along the minor and major axes of the elliptical FS can be observed with *s*- and *p*-polarized light [labeled α and α′ in Fig. 4 (A and B, respectively)]. To evaluate ε_F, we have fitted a parabola to the dispersions of the α and α′ bands, and the top positions of the dispersions as ε_F have been estimated to be ~ 8 meV for both bands of FeSe ($x = 0$), which demonstrates the reliability of the value of ε_F. The band top of the other hole band labeled β is located at 18 meV below E_F for $x = 0$. In Fig. 4C, we have plotted the substitution dependence of ε_F and the top positions of the β band.

The SC gap Δ has been determined from the raw EDCs at $k = \pm k_F$ and by fitting of the EDCs to a BCS spectral function (*18*). Justification for use of a BCS spectral function in the crossover region has been confirmed for the case of an ultracold atomic system (*19*). The fitting to the BCS spectral function has been conducted for $x = 0$ to 0.13, because the coherent peak becomes broader as *x* increases and the fitting becomes more difficult. The averaged values of Δ for $k = \pm k_F$ are plotted in Fig. 4D, in which the twofold symmetry of the electronic structure is taken into account. The values of Δ determined from both procedures show a similar substitution dependence, that is, they increase from $x = 0$ to $x = 0.04$ and decrease as *x* increases further. The substitution dependence of Δ/ε_F is shown in

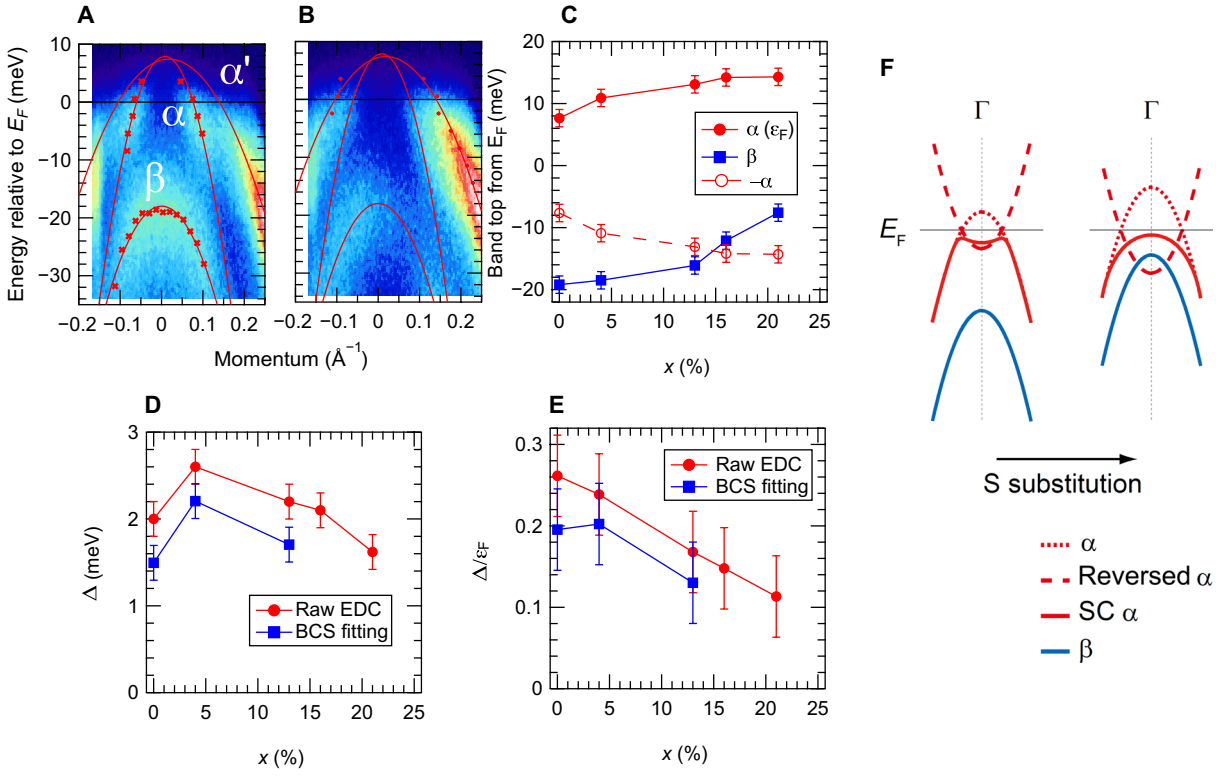

Fig. 4. Mechanism of the multiband BCS-BEC crossover in $FeSe_{1-x}S_x$. (**A**) ARPES intensity plot of FeSe along the Γ – *M* direction taken at 25 K with *s*-polarized light. The red markers are peak positions of the momentum distribution curves (MDCs) and EDCs corresponding to the dispersions of the α and β bands. The red curves are the results of parabola fitting. (**B**) Same as (A) but taken with *p*-polarized light. The red markers indicate the peak positions of the MDCs corresponding to the α′ band. (**C**) Substitution dependence of the top positions of the α and β bands determined from the fittings in (A) and (B). The sign-inverted one for the α band is also plotted. (**D**) Substitution dependence of Δ obtained from the raw EDCs at k_F and fitting by a BCS spectral function. (**E**) Substitution dependence of Δ/ε_F obtained in two ways as in (D). (**F**) Schematic image of the multiband BCS-BEC crossover in $FeSe_{1-x}S_x$. The solid red and blue curves represent the α and β bands in the SC state, respectively. The dashed red curve represents the α band inverted at $E = E_F$. The dotted curve represents the dispersion of the α band in the normal state.

Fig. 4E. A downward trend with increasing *x* can be recognized for both Δ curves determined from the raw EDCs and the fitting. For the electron band at the *M* point, the substitution dependence of Δ/ε_F should be similar to that of the hole band at the Γ point, because the substitution of S for Se is isovalent, and any carrier is not doped. In addition, taking account of the thermal conductivity, specific heat, and STS measurements (*14*, *15*), the SC gap at the electron band at the *M* point is expected to be very small for $x > 0.18$. Hence, Δ/ε for the electron band at the *M* point should be smaller than that of the hole band at the Γ point in this region.

DISCUSSION

As discussed in Figs. 2 and 3, the BQP band dispersions and the temperature dependence of the EDCs show the systematic evolutions to the BEC regime as *x* increases, and the system enters the BEC regime at $x = 0.21$. However, although two-dimensional mean field theory for a single-band system predicts that, when Δ/ε_F increases, the system moves toward the BEC regime (*20*), the experimental results for the substitution dependence of Δ/ε_F show that it decreases as *x* increases, as shown in Fig. 4E. This means that our results contradict the theory for a single-band system. Two possibilities to explain the BCS-BEC crossover in $FeSe_{1-x}S_x$ are discussed in the following.

The first possibility is the interband coupling between the hole band at the Γ point (α band) and the electron band at the *M* point. It has been proposed that, if the interband coupling between the hole and electron bands is strong enough, the hole band becomes BCS-like even if Δ/ε_F is close to unity (*21*). The present results may be explained if the strong interband coupling causes the BQP dispersion to exhibit a downward convex shape for $x = 0$ to 0.13, and this coupling becomes weak as *x* increases and the BQP dispersion becomes upward convex. However, we consider that the interband coupling between the hole and electron bands should be expected to be stronger for $x = 0.21$, because, in the nematic phase, the direction of the major axes is orthogonal between the elliptical hole and electron FS, and the nesting condition between the hole and electron FS becomes better for $x = 0.21$ owing to the absence of nematicity. Therefore, the substitution dependence of the interband coupling between these two bands at the Γ and *M* points is an unlikely explanation for the origin of the discrepancy.

The second and most plausible possibility is the interband coupling between the α and β bands in the SC state, which is tuned by nematicity. In case of $x = 0$ at low temperature, the energy difference between α and β band (d_{xz}/d_{yz}) is due to nematicity and spin-orbital coupling (*22*). As shown in Fig. 4C, as *x* increases, the energy difference between the α and β bands decreases. This is due to suppression of nematicity, because the α and β bands are mainly

contributed from the Fe 3*d* orbitals, and thus spin-orbit coupling in these bands should not change as x increases. In Fig. 4C, we have also plotted the sign-inverted value of the top position of the α band. The dispersion of the BQP band in the SC state can be regarded as the raw α band and its hypothetical inverted band with respect to E_F being hybridized by the particle-hole mixing. As schematically shown in Fig. 4F, whereas the inverted α band and the β band do not cross each other for $x = 0$, as x increases, they get to cross each other at $x = 0.16$, around the nematic QCP. When the inverted α and β bands are crossing, the interband coupling between these bands can be expected to become strong. As a result, the BQP band dispersion becomes upward convex, and the system enters a BEC regime. The sudden change of the SC state is observed at the nematic QCP (*14*, *15*), which is the same point as we observed in the BEC-like electronic structure. Theoretically, in a two-band model, when the interband coupling is weak, the preformed pairing region is suppressed compared to the single-band case, while it increases when the interband coupling becomes strong (*23*). We conclude that the suppression of nematicity controls the interband coupling of the α and β bands and the BCS-BEC crossover in the $FeSe_{1-x}S_x$ system, realizing the BEC state at $x = 0.21$.

MATERIALS AND METHODS

High-quality single crystals were grown by the chemical vapor transport method using $KCl/AlCl_3$ as the transport agent as described in (*24*). ARPES data were collected using a laser ARPES apparatus at ISSP with 6.994 eV, the sixth harmonics of an Nd:YVO_4 quasi–continuous-wave (repetition rate, 960 MHz) laser, and a VG-Scienta HR8000 electron analyzer as described in (*25*). This apparatus achieves a maximum energy resolution of 70 μeV and a lowest cooling temperature of 1.5 K, which enables direct measurement of the SC gap of $FeSe_{1-x}S_x$. The overall energy resolution was set to ~1.3 meV and the angular resolution was 0.1°. The Fermi edge of an evaporated gold film was measured to calibrate E_F energy positions. The error bars of the SC gap size were determined from the stability of the E_F position and were evaluated to be 200 μeV. More details on the accuracy of the measured gap size are described in previous reports (*25*, *26*). Polarization of the incident excitation laser was adjusted using half-wave (λ/2) and quarter-wave (λ/4) plates. Samples were cleaved in situ under ultrahigh vacuum and measurements were conducted at pressures of $< 5 \times 10^{-11}$ torr. The measurements were limited to the hole FS at the zone center owing to the relatively low excitation energy of 6.994 eV, with which the momentum around the electron FS at the zone corner cannot be accessed.

SUPPLEMENTARY MATERIALS

Supplementary material for this article is available at http://advances.sciencemag.org/cgi/content/full/6/45/eabb9052/DC1

REFERENCES AND NOTES

1. M. Randeria, E. Taylor, Crossover from Bardeen-Cooper-Schrieffer to Bose-Einstein condensation and the unitary fermi gas. *Annu. Rev. Condens. Matter Phys.* **5**, 209–232 (2014).
2. T. Shimojima, W. Malaeb, A. Nakamura, T. Kondo, K. Kihou, C.-H. Lee, A. Iyo, H. Eisaki, S. Ishida, M. Nakajima, S.-i. Uchida, K. Ohgushi, K. Ishizaka, S. Shin, Antiferroic electronic structure in the nonmagnetic superconducting state of the iron-based superconductors. *Sci. Adv.* **3**, e1700466 (2017).
3. H. Miao, T. Qian, X. Shi, P. Richard, T. K. Kim, M. Hoesch, L. Y. Xing, X.-C. Wang, C.-Q. Jin, J.-P. Hu, H. Ding, Observation of strong electron pairing on bands without Fermi surfaces in $LiFe_{1-x}Co_xAs$. *Nat. Commun.* **6**, 6056 (2015).
4. S. Rinott, K. B. Chashka, A. Ribak, E. D. L. Rienks, A. Taleb-Ibrahimi, P. Le Fevre, F. Bertran, M. Randeria, A. Kanigel, Tuning across the BCS-BEC crossover in the multiband superconductor $Fe_{1+y}Se_xTe_{1-x}$: An angle-resolved photoemission study. *Sci. Adv.* **3**, e1602372 (2017).
5. Y. Lubashevsky, E. Lahoud, K. Chashka, D. Podolsky, A. Kanigel, Shallow pockets and very strong coupling superconductivity in $FeSe_xTe_{1-x}$. *Nat. Phys.* **8**, 309–312 (2012).
6. F.-C. Hsu, J.-Y. Luo, K.-W. Yeh, T.-K. Chen, T.-W. Huang, P. M. Wu, Y.-C. Lee, Y.-L. Huang, Y.-Y. Chu, D.-C. Yan, M.-K. Wu, Superconductivity in the PbO-type structure α-FeSe. *Proc. Natl. Acad. Sci. U.S.A.* **105**, 14262–14264 (2008).
7. S. Kasahara, T. Watashige, T. Hanaguri, Y. Kohsaka, T. Yamashita, Y. Shimoyama, Y. Mizukami, R. Endo, H. Ikeda, K. Aoyama, T. Terashima, S. Uji, T. Wolf, H. von Löhneysen, T. Shibauchi, Y. Matsuda, Field-induced superconducting phase of FeSe in the BCS-BEC cross-over. *Proc. Natl. Acad. Sci. U.S.A.* **111**, 16309–16313 (2014).
8. S. Kasahara, T. Yamashita, A. Shi, R. Kobayashi, Y. Shimoyama, T. Watashige, K. Ishida, T. Terashima, T. Wolf, F. Hardy, C. Meingast, H. v. Löhneysen, A. Levchenko, T. Shibauchi, Y. Matsuda, Giant superconducting fluctuations in the compensated semimetal FeSe at the BCS-BEC crossover. *Nat. Commun.* **7**, 12843 (2016).
9. H. Takahashi, F. Nabeshima, R. Ogawa, E. Ohmichi, H. Ohta, A. Maeda, Superconducting fluctuations in FeSe investigated by precise torque magnetometry. *Phys. Rev. B* **99**, 060503 (2019).
10. A. Shi, T. Arai, S. Kitagawa, T. Yamanaka, K. Ishida, A. E. Böhmer, C. Meingast, T. Wolf, M. Hirata, T. Sasaki, Pseudogap behavior of the nuclear spin-lattice relaxation rate in FeSe probed by ^{77}Se-NMR. *J. Phys. Soc. Jpn.* **87**, 013704 (2018).
11. S. Rößler, C. Koz, L. Jiao, U. K. Rößler, F. Steglich, U. Schwarz, S. Wirth, Emergence of an incipient ordering mode in FeSe. *Phys. Rev. B* **92**, 060505(R) (2015).
12. T. Hanaguri, S. Kasahara, J. Böker, I. Eremin, T. Shibauchi, Y. Matsuda, Quantum vortex core and missing pseudogap in the multiband BCS-BEC crossover superconductor FeSe. *Phys. Rev. Lett.* **122**, 077001 (2019).
13. S. Hosoi, K. Matsuura, K. Ishida, H. Wang, Y. Mizukami, T. Watashige, S. Kasahara, Y. Matsuda, T. Shibauchi, Nematic quantum critical point without magnetism in $FeSe_{1-x}S_x$ superconductors. *Proc. Natl. Acad. Sci. U.S.A.* **113**, 8139–8143 (2016).
14. Y. Sato, S. Kasahara, T. Taniguchi, X. Xing, Y. Kasahara, Y. Tokiwa, Y. Yamakawa, H. Kontani, T. Shibauchi, Y. Matsuda, Abrupt change of the superconducting gap structure at the nematic critical point in $FeSe_{1-x}S_x$. *Proc. Natl. Acad. Sci. U.S.A.* **115**, 1227–1231 (2018).
15. T. Hanaguri, K. Iwaya, Y. Kohsaka, T. Machida, T. Watashige, S. Kasahara, T. Shibauchi, Y. Matsuda, Two distinct superconducting pairing states divided by the nematic end point in $FeSe_{1-x}S_x$. *Sci. Adv.* **4**, eaar6419 (2018).
16. B. Keimer, S. A. Kivelson, M. R. Norman, S. Uchida, J. Zaanen, From quantum matter to high-temperature superconductivity in copper oxides. *Nature* **518**, 179–186 (2015).
17. T. Hashimoto, Y. Ota, H. Q. Yamamoto, Y. Suzuki, T. Shimojima, S. Watanabe, C. Chen, S. Kasahara, Y. Matsuda, T. Shibauchi, K. Okazaki, S. Shin, Superconducting gap anisotropy sensitive to nematic domains in FeSe. *Nat. Commun.* **9**, 282 (2018).
18. K. Okazaki, Y. Ito, Y. Ota, Y. Kotani, T. Shimojima, T. Kiss, S. Watanabe, C.-T. Chen, S. Niitaka, T. Hanaguri, H. Takagi, A. Chainani, S. Shin, Superconductivity in an electron band just above the Fermi level: Possible route to BCS-BEC superconductivity. *Sci. Rep.* **4**, 4109 (2014).
19. J. P. Gaebler, J. T. Stewart, T. E. Drake, D. S. Jin, A. Perali, P. Pieri, G. C. Strinati, Observation of pseudogap behaviour in a strongly interacting Fermi gas. *Nat. Phys.* **6**, 569–573 (2010).
20. M. Randeria, J.-M. Duan, L.-Y. Shieh, Bound states, Cooper pairing, and Bose condensation in two dimensions. *Phys. Rev. Lett.* **62**, 981–984 (1989).
21. A. V. Chubukov, I. Eremin, D. V. Efremov, Superconductivity versus bound-state formation in a two-band superconductor with small Fermi energy: Applications to Fe pnictides/chalcogenides and doped $SrTiO_3$. *Phys. Rev. B* **93**, 174516 (2016).
22. M. D. Watson, A. A. Haghighirad, H. Takita, W. Mansuer, H. Iwasawa, E. F. Schwier, A. Ino, M. Hoesch, Shifts and splittings of the hole bands in the nematic phase of FeSe. *J. Phys. Soc. Jpn.* **86**, 053703 (2017).
23. H. Tajima, Y. Yerin, A. Perali, P. Pieri, Enhanced critical temperature, pairing fluctuation effects, and BCS-BEC crossover in a two-band Fermi gas. *Phys. Rev. B* **99**, 180503 (2019).
24. A. E. Böhmer, F. Hardy, F. Eilers, D. Ernst, P. Adelmann, P. Schweiss, T. Wolf, C. Meingast, Lack of coupling between superconductivity and orthorhombic distortion in stoichiometric single-crystalline FeSe. *Phys. Rev. B* **87**, 180505 (2013).
25. K. Okazaki, Y. Ota, Y. Kotani, W. Malaeb, Y. Ishida, T. Shimojima, T. Kiss, S. Watanabe, C.-T. Chen, K. Kihou, C. H. Lee, A. Iyo, H. Eisaki, T. Saito, H. Fukazawa, Y. Kohori, K. Hashimoto, T. Shibauchi, Y. Matsuda, H. Ikeda, H. Miyahara, R. Arita, A. Chainani, S. Shin, Octet-line node structure of superconducting order parameter in KFe_2As_2. *Science* **337**, 1314–1317 (2012).
26. Y. Ota, K. Okazaki, H. Q. Yamamoto, T. Yamamoto, S. Watanabe, C. Chen, M. Nagao, S. Watauchi, I. Tanaka, Y. Takano, S. Shin, Unconventional Superconductivity

in the BiS_2-based layered superconductor $NdO_{0.71}F_{0.29}BiS_2$. *Phys. Rev. Lett.* **118**, 167002 (2017).

Acknowledgments: We thank K. Adachi for valuable discussions. **Funding:** This research is supported by Grants-in-Aid for Scientific Research (KAKENHI) (grant numbers JP19H00651, JP19H01818, JP18H05227, JP19H00649, JP18H01177, JP18K13492, and JP20H02600) and Grants-in-Aid on Innovative Areas "Quantum Liquid Crystals" (grant numbers JP19H05824 and JP19H05826) and "Topological Material Science" (grant number JP15H05852) from the Japan Society for the Promotion of Science (JSPS). T.H. acknowledges the JSPS Research Fellowship for Young Scientists (DC2). **Author contributions:** T.H., Y.O., A.T., T.N., and A.F. performed the ARPES measurements. T.H. and K.O. analyzed the data. Samples were grown and characterized by S.K., Y.Ma, K.M., Y.Mi, and T.S. The manuscript was written by T.H. and K.O. All the authors discussed and contributed to the manuscript. S.S. and K.O. designed the project. **Competing interests:** The authors declare that they have no competing interests. **Data and materials availability:** All data needed to evaluate the conclusions in the paper are present in the paper and/or the Supplementary Materials. Additional data related to this paper may be requested from the authors.

Submitted 26 March 2020
Accepted 24 September 2020
Published 6 November 2020
10.1126/sciadv.abb9052

Citation: T. Hashimoto, Y. Ota, A. Tsuzuki, T. Nagashima, A. Fukushima, S. Kasahara, Y. Matsuda, K. Matsuura, Y. Mizukami, T. Shibauchi, S. Shin, K. Okazaki, Bose-Einstein condensation superconductivity induced by disappearance of the nematic state. *Sci. Adv.* **6**, eabb9052 (2020).